JACS
JOURNAL OF THE AMERICAN CHEMICAL SOCIETY
Cite This: J. Am. Chem. Soc. XXXX, XXX, XXX−XXX
Communication
pubs.acs.org/JACS

Enhanced Electron Transfer Mediated by Conjugated Polyelectrolyte and Its Application to Washing-Free DNA Detection

Seonhwa Park,[†,⊥] Ji-Eun Jeong,[‡,⊥] Van Sang Le,[‡] Jeongwook Seo,[†] Byeongjun Yu,[§] Da-Young Kim,[∥] Se-Hun Kwon,[∥] Sangyong Jon,[§] Han Young Woo,[*,‡] and Haesik Yang[*,†]

[†]Department of Chemistry and Chemistry Institute for Functional Materials, Pusan National University, Busan 46241, Korea
[‡]Department of Chemistry, Korea University, Seoul 02841, Korea
[§]Department of Biological Sciences, Korea Advanced Institute of Science and Technology (KAIST), Daejeon 34141, Korea
[∥]School of Materials Science and Engineering, Pusan National University, Busan 46241, Korea

Supporting Information

ABSTRACT: Direct electron transfer between a redox label and an electrode requires a short working distance (<1−2 nm), and in general an affinity biosensor based on direct electron transfer requires a finely smoothed Au electrode to support efficient target binding. Here we report that direct electron transfer over a longer working distance is possible between (i) an anionic π-conjugated polyelectrolyte (CPE) label having many redox-active sites and (ii) a readily prepared, thin polymeric monolayer-modified indium−tin oxide electrode. In addition, the long CPE label (∼18 nm for 10 kDa) can approach the electrode within the working distance after sandwich-type target-specific binding, and fast CPE-mediated oxidation of ammonia borane along the entire CPE backbone affords high signal amplification.

Direct electron transfer between a redox label and an electrode has been widely used for affinity biosensors.[1,2] Target-induced structural switching of an electrode-bound, redox-label-conjugated probe causes a large change in its rigidity and the distance between the electrode and the redox label, leading to a significant change in the electrochemical signal. This allows sensitive detection of small molecules and biomolecules even without a washing step. However, direct electron transfer between an electrode and a redox label is only measurable within a working distance of 1−2 nm because the electron transfer rate drops exponentially with increasing distance.[3,4] To meet these requirements, thin and low-defect self-assembled monolayers formed on clean and smooth Au electrodes are commonly used.[1,2] Moreover, it is challenging to apply direct electron transfer to versatile sandwich-type biosensors because it is difficult to place the redox label of an electrode-unbound diffusing probe in close proximity to an electrode via sandwich-type target-specific binding.

Interestingly, long-range electron transfer between an electrode and a diffusing redox-active species can be mediated by a metal nanoparticle, mainly as a result of the high density of states (i.e., numerous redox-active sites) of the metal nanoparticle.[3,5] However, when the distance between the electrode and metal nanoparticle exceeds ∼3 nm, the mediated electron transfer rate drops sharply, irrespective of the metal nanoparticle size.[3,5] In sandwich-type biosensors using metal nanoparticle labels, it is challenging to place a metal nanoparticle within a distance of ∼3 nm to an electrode because both the electrode and the metal nanoparticle are already covered by insulating layers (more than a few nm) constructed for target-specific binding.

Water-soluble π-conjugated polyelectrolytes (CPEs) are strongly visible-light-absorbing and fluorescent.[6,7] Specific binding of CPEs to target (bio)molecules leads to significant changes in absorbance and/or fluorescence, thus enabling sensitive and selective optical sensing and bioimaging. Importantly, one CPE has many redox-active sites that facilitate long-range direct electron transfers and high electrochemical signals.[8] We hypothesized that a long CPE label may readily approach an electrode closely, enabling direct electron transfer even in sandwich-type detection. Moreover, CPE-mediated electron transfer may occur along the entire CPE backbone.[9] Herein we report enhanced electron transfer mediated by a long, redox-active CPE label and demonstrate its utility for versatile washing-free sandwich-type detection.

To function as a redox label that allows a high signal-to-background ratio, an ideal CPE should have (i) high redox and/or electrocatalytic activity, (ii) high water solubility, (iii) long chain length (>10 nm), and (iv) low nonspecific adsorption. Figure 1a shows a p-type polymer backbone based on cyclopentadithiophene and thiophene (CDT_T)[10] that was employed to achieve facile electrochemical oxidation near 0 V vs Ag/AgCl. Anionic 4-sulfonatobutyl (SB) side chains were incorporated to obtain high water solubility[11] and low nonspecific adsorption. Hydrophilic triethylene glycol (TEG) side chains were added to decrease nonspecific adsorption and to improve the CPE redox activity.[12] A series of CPEs was synthesized by varying the feed ratio of the two monomers [CDT with SB side chains (CDT_SB, **1**) and CDT with TEG side chains (CDT_TEG, **3**)] (x:y) together with bis-stannylated thiophene (**2**) (Scheme S-1 in the Supporting Information (SI)). Five different random copolymers (P0, P1, P2, P3, P5, and P7) were prepared by Stille coupling (Figure 1a). For example, P3 was synthesized with x:y = 7:3. In addition, P3 was end-capped with 5-bromo-2-thiophenecarbox-

Received: November 23, 2017

DOI: 10.1021/jacs.7b12382
J. Am. Chem. Soc. XXXX, XXX, XXX−XXX

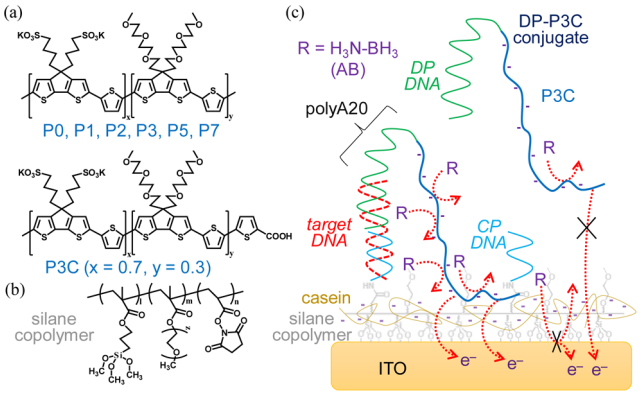

Figure 1. Molecular structures of (a) synthesized π-conjugated polyelectrolytes and (b) silane copolymer. (c) Schematic diagram of sandwich-type DNA detection using direct electron transfer.

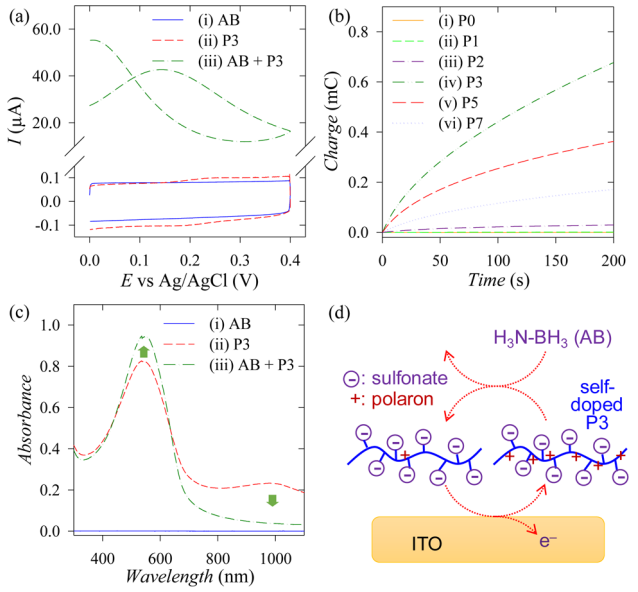

Figure 2. (a) Cyclic voltammograms obtained (at 20 mV/s) at ITO electrodes in PBS (pH 7.4) containing (i) 5.0 mM AB, (ii) 10 μg/mL P3, and (iii) 5.0 mM AB and 10 μg/mL P3. (b) Chronocoulograms obtained (at 0.1 V) at ITO electrodes in PBS containing 5.0 mM AB and 10 μg/mL CPE [(i) P0, (ii) P1, (iii) P2, (iv) P3, (v) P5, or (vi) P7]. (c) UV/vis absorbance obtained in PBS containing (i) 5.0 mM AB, (ii) 50 μg/mL P3, and (iii) 5.0 mM AB and 50 μg/mL P3. (d) Schematic diagram of P3-mediated AB oxidation.

ylic acid to prepare carboxylic acid-terminated P3C (Figure 1a). The synthesized CPEs were separated using a centrifugal filter with a molecular weight cutoff of 10 kDa. The absorption spectra suggest that the low-molecular-weight monomers and oligomers were removed by this process (Figure S-1). Amine-terminated detection probe (DP) DNA was conjugated with carboxylic acid-terminated P3C to prepare a DP−P3C conjugate (Figure 1c). This conjugation was confirmed by gel electrophoresis (Figure S-2).

To obtain a high signal-to-background ratio, the mediated oxidation of a reductant by the CPE should be very fast, whereas the direct oxidation of the reductant at an electrode should be very slow. To meet these requirements, the mediated and direct oxidation of five strong reductants was tested at an indium tin oxide (ITO) electrode having a low electrocatalytic activity (Figures 2a and S-3). Among the five reductants, ammonia borane ($H_3N{-}BH_3$, AB) showed the highest P3-mediated oxidation current and the lowest direct oxidation current. The cyclic voltammogram obtained in phosphate-buffered saline (PBS, pH 7.4) containing AB (curve i in Figure 2a) was in good agreement with that in PBS, indicating that direct oxidation of AB is very slow at the ITO electrode.

Low currents of P3 oxidation were observed from ~0.15 V (curve ii in Figure 2a). However, the anodic currents increased immensely in the presence of AB (curve iii in Figure 2a) as a result of fast P3-mediated AB oxidation. Additionally, the redox and electrocatalytic activity was found to depend on the feed ratio of CDT_SB to CDT_TEG. As expected from previous reports,[12] the redox and electrocatalytic activities varied as the CDT_TEG ratio increased, with P3 providing the highest electrochemical signals among the six CPEs (Figure 2b). P3C also showed high electrocatalytic activity toward AB oxidation (Figure S-4). Therefore, P3C was chosen as a redox label for sensitive DNA detection. It should be noted that an applied potential of 0.1 V yielded the highest signal-to-background ratio (Figure S-5).

The absorption spectra of P3 obtained in PBS in the absence and presence of AB are provided in Figure 2c. In the absence of AB, two absorption bands were observed, centered at 560 and 1000 nm. The first band is characteristic of π-conjugated polymer absorption, and the second one is due to absorption by polarons.[13] The presence of the second band indicates that P3 was self-doped.[13,14] Interestingly, the absorbance of the second band decreased in the presence of AB whereas that of the first band increased. This absorbance change indicates that the concentration of positive polarons in P3 decreased. P3C also showed a similar absorbance change by AB (Figure S-6). Figure 2d shows that the self-doped, oxidized P3 is reduced by AB, and the resultant (reduced) P3 is then electrochemically oxidized and rereduced by AB.

A silane copolymer containing a silane group, a poly(ethylene glycol) group, and an ester group (Figure 1b) was used (i) to form a polymeric self-assembled monolayer on an ITO electrode, (ii) to inhibit nonspecific adsorption, and (iii) to immobilize an amine-terminated capture probe (CP) DNA (Figure 1c).[15] To further inhibit nonspecific adsorption of the negatively charged DP−P3C conjugate, the sensing electrode was treated with negatively charged casein (Figure 1c). The polymeric monolayer and casein can inhibit direct electron transfer between the electrode and the DP−P3C conjugate. Since the polymeric monolayer thickness is ~1 nm,[16] the electrode was also covered with CP DNA, and the penetration of long and negatively charged P3C through pinholes of the insulating layers might not be easy, more facile long-range direct electron transfer (>1 nm) is required to obtain high electrochemical signals. Such electron transfer may be possible with long P3C because it has many redox-active sites.

To investigate this possibility, the ITO electrode was coated with a 1 nm thick, pinhole-free Al_2O_3 film by atomic layer deposition.[4] Figure 3a shows that the fast redox reaction of ferrocenemethanol (FcMeOH) at a bare ITO electrode was significantly inhibited at an Al_2O_3/ITO electrode. However, when P3 was present on the Al_2O_3/ITO electrode, the redox reaction was substantially accelerated. This phenomenon was also observed with redox reactions of $Ru(NH_3)_6^{3+}$ and AB (Figure S-7). All of these results reveal that the P3-mediated electron transfer is faster than the direct electron transfer between the small redox-active species FcMeOH and the electrode (Figure 3b). These results clearly show that direct

DOI: 10.1021/jacs.7b12382
J. Am. Chem. Soc. XXXX, XXX, XXX−XXX

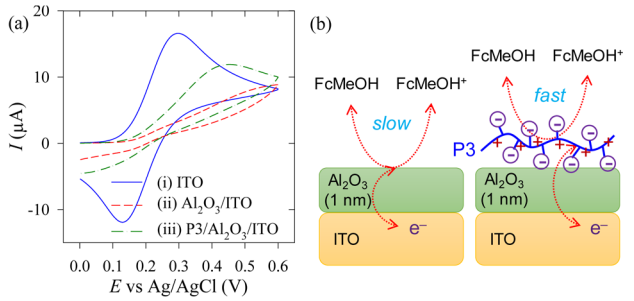

Figure 3. (a) Cyclic voltammograms obtained (at 20 mV/s) in phosphate buffer (pH 7.0) containing 1.0 mM ferrocenemethanol (FcMeOH) at the (i) bare ITO electrode, (ii) Al_2O_3/ITO electrode, and (iii) P3-adsorbed Al_2O_3/ITO (P3/Al_2O_3/ITO) electrode. (b) Schematic diagrams of direct and P3-mediated oxidation of FcMeOH.

electron transfer between P3 and the electrode over a longer working distance is possible.

Nonspecific adsorption of proteins to P3 readily occurs because the CDT_T backbone is hydrophobic.[17] Figure 4a shows that the adsorption of bovine serum albumin (BSA) to P3 significantly reduced the redox and electrocatalytic activities shown in Figure 2a. However, addition of the nonionic surfactant Tween-20 recovered the electrocatalytic activity of P3 considerably (curve iii in Figure 4a). The chronocoulometric data in Figure S-8 confirm the unfavorable effect of BSA and the favorable effect of Tween-20. The hydrophobic alkyl side chain of Tween-20 becomes adsorbed on the CDT_T backbone, and the oligo(ethylene glycol)s of Tween-20 minimize the adsorption of BSA.

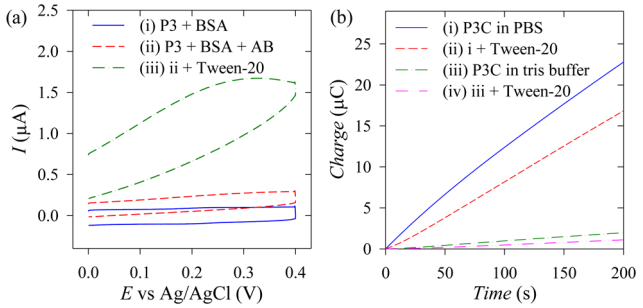

Figure 4. (a) Cyclic voltammograms obtained (at 20 mV/s) at ITO electrodes in PBS containing (i) 10 μg/mL P3 and 1.0% BSA; (ii) P3, BSA, and 5.0 mM AB; and (iii) P3, BSA, AB, and 0.05% Tween-20. (b) Chronocoulograms obtained (at 0.1 V) at a casein/silane copolymer/ITO electrode in PBS containing (i) 10 μg/mL P3C and 5.0 mM AB and (ii) P3C, AB, and 0.05% Tween-20 and in Tris buffer (20 mM, pH 7.5) containing (iii) 10 μg/mL P3C and 5.0 mM AB and (iv) P3C, AB, and 0.05% Tween-20.

Nonspecific adsorption of P3 to an ITO electrode modified with a silane monolayer decreased significantly in PBS after its additional modification with casein (Figure S-9). However, for P3C, its nonspecific adsorption to the casein/silane copolymer/ITO electrode was not negligible in PBS (curve i in Figure 4b). When Tween-20 was added in PBS, the nonspecific adsorption decreased slightly (curve ii in Figure 4b). Importantly, the nonspecific adsorption was much lower in Tris buffer (pH 7.5) (curves iii and vi in Figure 4b) than in PBS. The positively charged ammonium ion of Tris may interact electrostatically with the negatively charged P3C and electrode, alleviating their nonspecific interaction.

Finally, the redox label P3C was applied to DNA detection of the *BRCA1* gene.[18] Target DNA was hybridized twice with the CP DNA on the electrode and the DP−P3C conjugate in solution (Figure 1c). Given that the length of the 31 base pair region corresponds to ca. 10 nm, that the DP−P3C conjugate contains a flexible spacer of 20 adenines (polyA20) (Figure 1c), and that the length of the fully stretched 10 kDa P3C is ∼18 nm (see the SI), it is expected that P3C closely approaches the electrode after sandwich-type target-specific binding. In washing-free sandwich-type detection, the electrocatalytic reaction of the unhybridized DP−P3C conjugate in solution can increase the background level. However, this contribution was negligible because the direct electron transfer between P3C and the electrode may occur within 3−5 nm and the concentration of the unhybridized DP−P3C conjugate was low (Figure 1c; also see the SI). Since P3C is electrically conductive, electron transfer and P3C-mediated AB oxidation readily occur along the entire P3C backbone.

Washing-free DNA detection was performed in Tris buffer (pH 7.5) containing Tween-20 and $MgCl_2$. This buffer condition is commonly used for rolling-circle amplification that generates highly amplified ssDNA. Chronocoulograms were recorded after only 30 min of incubation without a washing step (Figure 5a). The calculated detection limit was ca. 10 pM (Figure 5b), and the dynamic range was very large (for possible reasons, see the SI). Importantly, a low detection limit was achieved without a washing step.

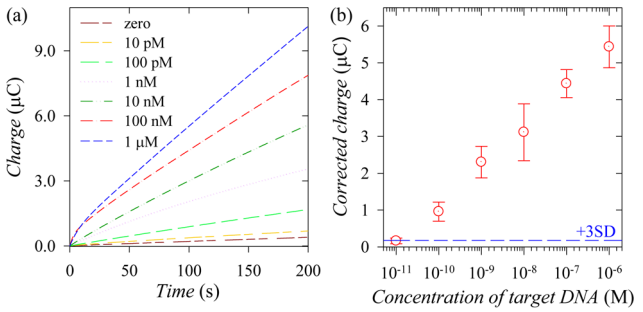

Figure 5. (a) Chronocoulograms obtained (at 0.1 V) using washing-free DNA detection (Figure 1c) for different concentrations of target DNA in Tris buffer (40 mM, pH 7.5) containing 0.05% Tween-20, 50 mM KCl, 10 mM $MgCl_2$, and 5 mM $(NH_4)_2SO_4$. (b) Calibration plot of the charges measured at 100 s in the chronocoulograms in (a) (see the SI for details).

In summary, three phenomena enabled us to obtain a high electrochemical signal: (i) the electron transfer between a P3C label and an electrode provides a longer working distance; (ii) the long P3C label approaches the electrode within the working distance after sandwich-type binding; and (iii) the fast P3C-mediated oxidation of AB along the entire P3C backbone affords high signal amplification.

■ ASSOCIATED CONTENT

Ⓢ Supporting Information

The Supporting Information is available free of charge on the ACS Publications website at DOI: 10.1021/jacs.7b12382.

Experimental procedures, UV/vis data, gel electrophoresis results, electrochemical data for five reductants, dependence on an applied potential, control data for nonspecific binding and selective hybridization, and DNA detection in PBS and serum (PDF)

DOI: 10.1021/jacs.7b12382
J. Am. Chem. Soc. XXXX, XXX, XXX−XXX

AUTHOR INFORMATION

Corresponding Authors

*hyang@pusan.ac.kr
*hywoo@korea.ac.kr

ORCID

Sangyong Jon: 0000-0002-6971-586X
Han Young Woo: 0000-0001-5650-7482
Haesik Yang: 0000-0001-7450-5915

Author Contributions

⊥S.P. and J.-E.J. contributed equally.

Notes

The authors declare no competing financial interest.

ACKNOWLEDGMENTS

This work was supported by the Samsung Research Funding Center of Samsung Electronics (Project SRFC-TA1503-01) and the National Research Foundation of Korea (2017M3A7B4041973 and 2015R1D1A1A09056905).

REFERENCES

(1) Lubin, A. A.; Plaxco, K. W. *Acc. Chem. Res.* **2010**, *43*, 496.
(2) Li, D.; Song, S.; Fan, C. *Acc. Chem. Res.* **2010**, *43*, 631.
(3) Chazalviel, J.-N.; Allongue, P. *J. Am. Chem. Soc.* **2011**, *133*, 762.
(4) Lee, H.; Chang, B.-Y.; Kwack, W.-S.; Jo, K.; Jeong, J.; Kwon, S.-H.; Yang, H. *J. Electroanal. Chem.* **2013**, *700*, 8.
(5) Barfidokht, A.; Ciampi, S.; Luais, E.; Darwish, N.; Gooding, J. J. *Anal. Chem.* **2013**, *85*, 1073.
(6) Duarte, A.; Pu, K.-Y.; Liu, B.; Bazan, G. C. *Chem. Mater.* **2011**, *23*, 501.
(7) Zhan, R.; Liu, B. *Chem. Rec.* **2016**, *16*, 1715.
(8) Casado, N.; Hernández, G.; Sardon, H.; Mecerreyes, D. *Prog. Polym. Sci.* **2016**, *52*, 107.
(9) Winther-Jensen, B.; MacFarlane, D. R. *Energy Environ. Sci.* **2011**, *4*, 2790.
(10) Scaria, R.; Ali, F.; Dhawan, S. K.; Chand, S. *J. Mater. Sci.* **2015**, *50*, 555.
(11) Patil, A. O.; Ikenoue, Y.; Wudl, F.; Heeger, A. J. *J. Am. Chem. Soc.* **1987**, *109*, 1858.
(12) Roncali, J.; Shi, L. H.; Garreau, R.; Garnier, F.; Lemaire, M. *Synth. Met.* **1990**, *36*, 267.
(13) Mai, C.-K.; Zhou, H.; Zhang, Y.; Henson, Z. B.; Nguyen, T.-Q.; Heeger, A. J.; Bazan, G. C. *Angew. Chem., Int. Ed.* **2013**, *52*, 12874.
(14) Mai, C.-K.; Arai, T.; Liu, X.; Fronk, S. L.; Su, G. M.; Segalman, R. A.; Chabinyc, M. L.; Bazan, G. C. *Chem. Commun.* **2015**, *51*, 17607.
(15) Park, S.; Lee, K.-B.; Choi, I. S.; Langer, R.; Jon, S. *Langmuir* **2007**, *23*, 10902.
(16) Jon, S.; Seong, J.; Khademhosseini, A.; Tran, T.-N. T.; Laibinis, P. E.; Langer, R. *Langmuir* **2003**, *19*, 9989.
(17) Pu, K.-Y.; Liu, B. *J. Phys. Chem. B* **2010**, *114*, 3077.
(18) Dunning, A. M.; Chiano, M.; Smith, N. R.; Dearden, J.; Gore, M.; Oakes, S.; Wilson, C.; Stratton, M.; Peto, J.; Easton, D.; Clayton, D.; Ponder, B. A. *Hum. Mol. Genet.* **1997**, *6*, 285.

DOI: 10.1021/jacs.7b12382
J. Am. Chem. Soc. XXXX, XXX, XXX−XXX